



Detection feasibility of the stochastic gravitational wave background from cosmic strings

Sam Wikeley, University of Glasgow

September 5, 2018

Abstract

With the next generation of gravitational wave observatories under development, the feasibility of a detection of the stochastic gravitational wave background (SGWB) has garnered much interest. In order to assess the possibility of such a detection, sensitivity curves for a given detector must be generated to allow for a comparison with the SGWB signal. Due to the broadband nature of a SGWB signal, a large improvement in sensitivity can be generated by including an additional integration over frequency in the calculation of a detector's sensitivity curve. This results in a power-law integrated sensitivity curve, the construction of which will be outlined in this report, with results presented for the LIGO, LISA, Einstein Telescope, and Cosmic Explorer experiments. These curves will then be compared with the SGWB signal produced by a scaling cosmic string network, the theory and construction of which will be discussed.

Contents

- 1. Introduction** **3**

- 2. The Stochastic Gravitational Wave Background** **3**

- 3. Power-law Integrated Sensitivity Curves** **4**
 - 3.1. Theory 4
 - 3.2. Construction 5

- 4. GW Backgrounds from Cosmic String Networks** **8**
 - 4.1. Theory 8
 - 4.2. Comparison with Detector Sensitivities 11

- 5. Conclusions and Outlook** **12**

- A. Appendix** **16**

1. Introduction

The detection of gravitational waves (GW) by the LIGO collaboration in 2015 ushered in a new era of astronomy, allowing for the first time the possibility of the simultaneous use of electromagnetic and gravitational radiation in the study of astrophysical phenomena. The gravitational waves observed in this case were produced during the merging of two black holes, approximately 1.3 billion years ago, and since this initial detection, many other transient events have been observed. As the field of gravitational wave astronomy continues to develop, and the possibilities of this new form of observation are explored, much attention has been focused on the detection of the stochastic gravitational wave background (SGWB). Much like the cosmic microwave background, it is thought that there should exist a background of gravitational waves produced by a large number of independent events during the early universe, with also a contribution from the many astrophysical sources that have occurred since this epoch, for which the gravitational signals emitted are too weak to resolve individually [1]. The detection of such a background would have a profound impact on the field of early-universe cosmology, providing an unprecedented window into the mechanisms of high-energy physics a fraction of a second after the big bang, an era in which gravitational radiation is the only direct messenger available. For this reason, one of the main aims of the next generation of gravitational wave observatories is the detection of the SGWB, the feasibility of which will be the main focus of this report.

In section 2, the stochastic gravitational wave background will be introduced, with a discussion of the relevant properties and characterisation. Section 3 will focus on the theory and construction of power-law integrated sensitivity curves for gravitational wave detectors, the results of which will be presented for the LISA, LIGO, Einstein Telescope (ET), and Cosmic Explorer (CE) experiments. In section 4 the production of gravitational waves from a network of cosmic strings will be outlined, and the resulting theoretical SGWB signal will be plotted against the power-law integrated sensitivity curves, allowing the feasibility of detection to be assessed. Finally, section 5 will feature the conclusions of this work.

2. The Stochastic Gravitational Wave Background

Gravitational waves, first postulated in the early 20th century, are propagating disturbances in the fabric of spacetime, produced by accelerating masses. They arise naturally from the theory of general relativity via the linearisation of Einstein's field equations, resulting in a wave equation with a propagation speed equal to that of light [1]. A stochastic background of gravitational waves is formed from a superposition of these waves with all possible propagation directions [1]. It is expected that, to a good approximation, the SGWB will be isotropic, stationary, and unpolarised [2]. These factors prescribe that it is possible to uniquely define a SGWB via a single frequency dependent function; however, the specific choice of such a characterisation is context dependent,

and requires the introduction of a number of parameters.

To begin, the dimensionless quantity $\Omega_{gw}(f)$ is defined to be [3]:

$$\Omega_{gw}(f) = \frac{1}{\rho_c} \frac{d\rho_{gw}}{d \ln f}. \quad (1)$$

Here ρ_{gw} is the energy density of the SGWB, f is frequency, and ρ_c is the total energy density of the universe for which the spatial geometry is flat, known as the critical density. In natural units, ρ_c is

$$\rho_c = \frac{3H_0^2}{8\pi G}, \quad (2)$$

where G is Newton's constant and H_0 is the present value of the Hubble constant, conventionally defined to be $H_0 = h_0 \times 100 \text{ km}/(\text{s} \times \text{Mpc})$, with h_0 parameterising the current experimental uncertainty. To remove the dependence on this uncertainty it is conventional to multiply Eq. (1) through by h_0^2 , thereby resulting in a characterisation of the spectrum with the quantity $h_0^2\Omega_{gw}(f)$. Physically, this parameter describes the fractional contribution of the energy density of the gravitational waves, within some frequency range, to the total energy required to close the universe [3]. For the remainder of this report, the spectrum will be characterised in terms of the quantity $h_0^2\Omega_{gw}(f)$, however it is useful to make note of another parameter that appears frequently throughout the literature, the spectral density $S_h(f)$, which can be converted to via the expression [4]:

$$S_h(f) = \frac{3H_0^2}{2\pi^2} \frac{\Omega_{gw}(f)}{f^3}. \quad (3)$$

With these quantities a direct comparison of a SGWB signal to the noise within a detector can be made, allowing the feasibility of a detection of the SGWB for a given signal-to-noise ratio to be assessed.

3. Power-law Integrated Sensitivity Curves

3.1. Theory

In order to assess the feasibility of a SGWB detection with a given detector, typically the properties of the detector are used to construct a sensitivity curve in terms of a chosen characterisation, which can then be compared with the theoretical signal from a source. Considering the characterisation of the signal in terms of $h_0^2\Omega_{gw}(f)$, if for a given range of frequencies the value of $h_0^2\Omega_{gw}(f)$ is greater for the theoretical signal, than that of the detector sensitivity, then the signal has a signal-to-noise ratio (SNR) that is greater than one [4]. This method can be applied to both the detection of transient

gravitational waves signals and the stochastic background; however, in the latter case it can be shown that a significant increase in the sensitivity can be achieved by performing an additional integration over frequency. This improvement arises due to the broadband nature of a SGWB signal, as it can be shown that the SNR scales linearly with $\sqrt{N_{\text{bins}}}$, where N_{bins} is the number of frequency bins of width δf , within a total bandwidth Δf , resulting in the relation [4]:

$$N_{\text{bins}} = \frac{\Delta f}{\delta f} . \quad (4)$$

As the proportionality constant in this case depends on the spectral shape of the background, the improvement to the sensitivity generated by this consideration is signal dependent, and is therefore not necessarily accounted for in the sensitivity curve of a detector [4]. For the case in which the SGWB can be characterised with a power-law frequency dependence, it is possible to take these factors into account via the construction of power-law integrated sensitivity curves, first developed in [4].

3.2. Construction

Given the assumed properties of the SGWB outlined in section 2, the signal-to-noise ratio for a background is given by [5]:

$$\text{SNR} = \sqrt{T \int_{f_{\text{min}}}^{f_{\text{max}}} df \left[\frac{h^2 \Omega_{\text{gw}}(f)}{h^2 \Omega_{\text{sens}}(f)} \right]^2} , \quad (5)$$

where f is frequency, T is the observation time of the detector, $h^2 \Omega_{\text{sens}}(f)$ describes the detector sensitivity, and $h^2 \Omega_{\text{gw}}(f)$ quantifies the SGWB signal. For notational convenience the subscript on h_0 has been dropped, as will be done for the remainder of this report. As stated previously, the construction of a power-law integrated sensitivity curve for a given detector requires that the SGWB signal can be expressed as a power-law spectrum. This spectrum is defined as:

$$\Omega_{\text{gw}}(f) = \Omega_{\beta} \left(\frac{f}{f_{\text{ref}}} \right)^{\beta} , \quad (6)$$

where β is the spectral index, Ω_{β} is the amplitude, and f_{ref} is a reference frequency, the choice of which is arbitrary [4]. Substituting this expression into Eq. (5) results in

$$\Omega_{\beta} = \frac{\text{SNR}}{\sqrt{T}} \left(\int_{f_{\text{min}}}^{f_{\text{max}}} df \left[\frac{h^2}{h^2 \Omega_{\text{sens}}(f)} \left(\frac{f}{f_{\text{ref}}} \right)^{\beta} \right]^2 \right)^{-\frac{1}{2}} , \quad (7)$$

which can subsequently be entered into Eq. (6) to obtain

$$h^2\Omega_{\text{gw}}(f) = f^\beta \frac{\text{SNR}}{\sqrt{T}} \left(\int_{f_{\text{min}}}^{f_{\text{max}}} df \left[\frac{f^\beta}{h^2\Omega_{\text{sens}}(f)} \right]^2 \right)^{-\frac{1}{2}}, \quad (8)$$

where the expression has been multiplied through by h^2 to remain within the characterisation outlined previously. Equation (8) defines a series of power-law curves with β setting the spectral index. By plotting this expression for a series of β and a specified SNR, and subsequently computing the envelope of the generated curves, the power-law integrated sensitivity curve is obtained. Formally, this curve is therefore defined by $h^2\Omega_{\text{PL}}(f)$, where

$$h^2\Omega_{\text{PL}}(f) = \max_{\beta} \left[f^\beta \frac{\text{SNR}}{\sqrt{T}} \left(\int_{f_{\text{min}}}^{f_{\text{max}}} df \left[\frac{f^\beta}{h^2\Omega_{\text{sens}}(f)} \right]^2 \right)^{-\frac{1}{2}} \right]. \quad (9)$$

An example of the results of this method can be seen in Figure 1, which shows the power-law integrated sensitivity curve for the LISA experiment, using an SNR of 10 and an operation time of 4 years, 75% of which has been taken to be uptime. In order to generate the power-laws, 30 values of β have been used, within the range $\beta \in [-7, 7]$. Furthermore, Figure 2 shows the effect of changing the SNR in the generation of the power-law integrated sensitivity curve for LISA, once again using an operation time of 4 years, and Figure 3 shows the dependence of the curve on the operation time, using a constant SNR of 10.

The significance of Figure 1 can be understood as follows. Any lines that are tangent to the power-law integrated sensitivity curve represent a contribution to a SGWB power-law spectrum with an SNR of 10 [4]. Consequently, by comparing a curve corresponding to a predicted background with this new sensitivity curve, information about the background's SNR range is obtained. If the background curve lies below the power-law integrated sensitivity curve at all frequencies, then the background has an SNR that is less than that with which the sensitivity curve was generated, which in this case is an SNR of 10. Conversely, if the background curve lies above the sensitivity curve for a given frequency range, then within this range the background will be observable with an SNR greater than 10.

The construction of a power-law integrated sensitivity curve for an experiment such as LIGO is slightly more involved than for LISA, due to the fact that LIGO requires the correlation of two detectors. In this case, the SNR equation, Eq. (5), is modified to be:

$$\text{SNR} = \sqrt{T \int_{f_{\text{min}}}^{f_{\text{max}}} df \left[\Gamma(f) \frac{h^2\Omega_{\text{gw}}(f)}{h^2\Omega_{\text{sens}}(f)} \right]^2}, \quad (10)$$

where the function $\Gamma(f)$ is given by [2]

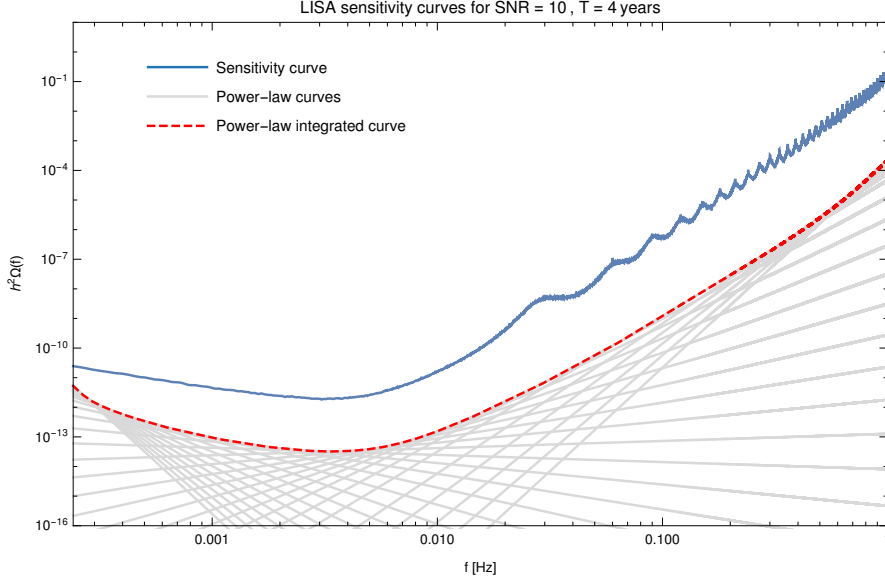


Figure 1: Sensitivity curves for the LISA experiment. The blue curve shows the detector sensitivity, the grey lines are the power-law curves generated for an SNR of 10 and an operation time of 4 years, and the red curve is the envelope of the power-law curves, hence representing the power-law integrated sensitivity curve. The power-law curves have been generated for 30 values of β , within the range $\beta \in [-7, 7]$.

$$\Gamma(f) = \int \frac{d\hat{\Omega}}{4\pi} \left[\sum_A F_1^A(\hat{\Omega}) F_2^A(\hat{\Omega}) \right] \exp \left(2\pi i f \hat{\Omega} \cdot \frac{\Delta\vec{x}}{c} \right). \quad (11)$$

Here polar coordinates are used with $\hat{\Omega} = (\sin\theta \sin\phi, \sin\theta \cos\phi, \cos\theta)$, and $\Delta\vec{x}$ is the separation between the two detectors. The functions $F_1^A(\hat{\Omega})$ and $F_2^A(\hat{\Omega})$ are pattern functions which take into account the geometry of the detectors, with the subscript representing the detector and the superscript, $A = +, \times$, signifying the gravitational wave polarisation. For the purposes of this report, instead of an explicit calculation of Eq. (11), data for the overlap reduction function, $\gamma(f)$, for LIGO was taken from [4], and converted to $\Gamma(f)$ via the relation:

$$\Gamma(f) = F_{12} \gamma(f), \quad (12)$$

where $F_{12} = 2/5$ for the correlation of two interferometers [2]. The resulting power-law integrated sensitivity curves for LIGO, as well as those generated for Einstein Telescope and Cosmic Explorer, which do not require the inclusion of $\Gamma(f)$, can be seen in Appendix A.

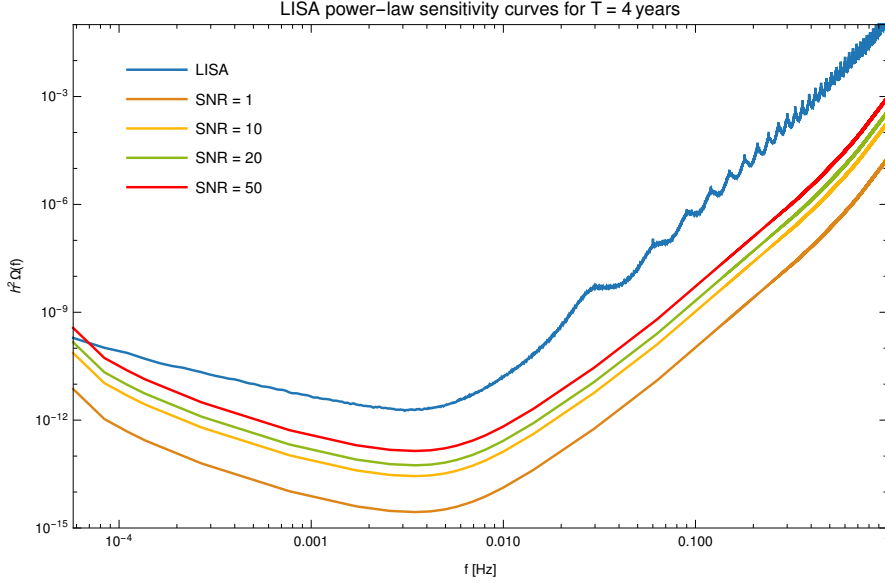


Figure 2: Power-law integrated sensitivity curves for the LISA experiment, generated for four values of SNR and an operation time of 4 years. The blue curve is the LISA sensitivity curve, while the orange, yellow, green, and red curves are the power-law integrated sensitivity curves for SNR values of 1, 10, 20, and 50 respectively.

4. GW Backgrounds from Cosmic String Networks

At present, there are a number of primordial mechanisms that are thought to have contributed to the SGWB. These broadly fall into three main categories: gravitational waves that are emitted from processes associated with inflation, first-order phase transitions, and cosmic strings; however, for the purpose of this report, only the contributions from cosmic strings will be considered. This section will provide a brief introduction to the mechanisms by which gravitational waves are emitted from a scaling cosmic string network, and an outline of the construction of energy density curves for the resulting signal.

4.1. Theory

Cosmic strings arise in many extensions of the Standard Model as scalar or gauge fields with an energy density that is concentrated along a one-dimensional line [6]. It is thought that symmetry-breaking phase transitions in the early universe may have given rise to entire networks of cosmic strings, featuring both infinitely long and closed loop strings. Soon after the formation of such a network, the strings reach a point at which their total energy density evolves with the net cosmological energy density, with a relative fraction $G\mu$, where G is Newton's constant and μ is the string tension [7]. At this point, the

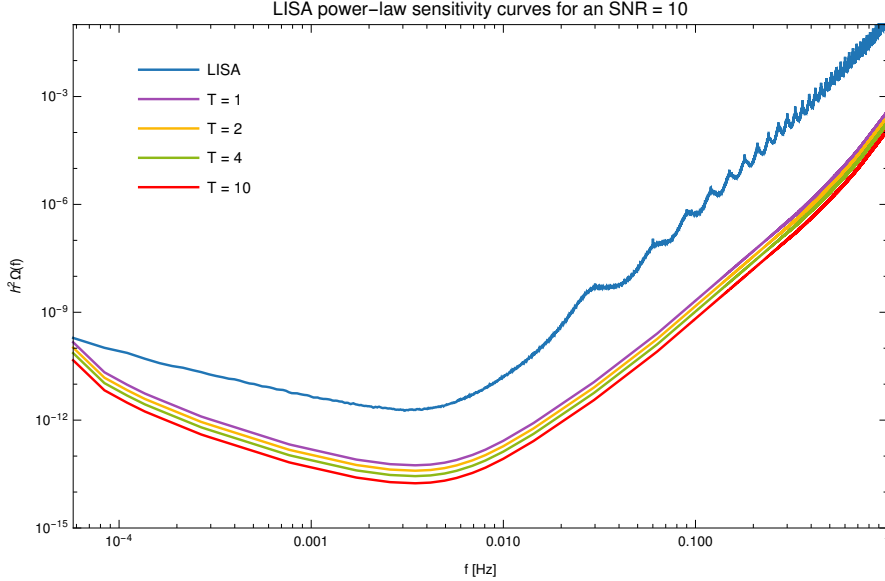


Figure 3: Power-law integrated sensitivity curves for the LISA experiment, generated for an SNR of 10 and four different operation times. The blue curve is the LISA sensitivity curve, while the purple, yellow, green, and red curves are the power-law integrated sensitivity curves for operation times of 1, 2, 4, and 10 years respectively.

network consists primarily of closed string loops with a small number of strings with Hubble length, which are interpreted as being infinitely long [7]. As time increases, the network expands with the universe, causing the infinitely long strings to intersect and split, forming new closed loops which then oscillate with a frequency proportional to the inverse of their radius, and decay via the emission of gravitational radiation [8].

Idealised Nambu-Goto strings are a useful class of strings to study as in this case gravitational waves are the dominant form of radiation emission [7]. Furthermore, during the scaling process outlined above, it is thought that the main contribution to the gravitational wave spectrum emitted by these strings will be due to the oscillation of closed loops, and hence this will be the case considered here [9]. Due to these considerations, the SGWB will be dependent on the rate of loop production, given by

$$\frac{dn}{dt_i} = \frac{0.1C_{eff}(t_i)}{\alpha t_i^4}, \quad (13)$$

where n is the number of loops, t_i is the time at which the loop is formed, and α is a constant loop size parameter which quantifies the size of the loop relative to the horizon [9]. $C_{eff}(t_i)$ is a function dependent on the dominant energy density of the universe at time t_i , known as the loop emission factor, which takes values of $C_{eff} = 5.4, 0.39$ for

radiation and matter domination respectively [7]. A closed loop produced at time t_i will have a length l that evolves via the expression:

$$l(t) = \alpha t_i - \Gamma G\mu (t - t_i) , \quad (14)$$

where Γ characterises the shrinking of the loop size due to gravitational wave emission [9]. The loop will lose energy at a constant rate, with a total energy loss comprised of a set of normal-mode oscillations at frequencies [9]

$$f_k = \frac{2k}{l} , \quad k \in \mathbb{Z}^+ . \quad (15)$$

Once the gravitational waves are emitted, they are redshifted at a rate inversely proportional to the cosmological scale factor, $a(t)$ [9]. By substituting Eq. (14) into Eq. (15) and taking the redshift into account, an expression for the frequency of a gravitational wave observed at present time, t_0 , is obtained [9]:

$$f = \frac{a(\tilde{t})}{a(t_0)} \frac{2k}{\alpha t_i - \Gamma\mu(\tilde{t} - t_i)} , \quad (16)$$

where \tilde{t} is the time at which the gravitational wave is emitted. Combining these factors, the gravitational wave signal from a cosmic string network can be stated by summing over the contribution from each mode [7]:

$$h^2\Omega_{CS}(f) = \frac{h^2}{\rho_c} \sum_k \frac{2k}{f} \frac{0.1\Gamma_k G\mu^2}{\alpha(\alpha + \Gamma G\mu)} \int_{t_F}^{t_0} d\tilde{t} \frac{C_{eff}(t_i)}{t_i^4} \left[\frac{a(\tilde{t})}{a(t_0)} \right]^5 \left[\frac{a(t_i)}{a(\tilde{t})} \right]^3 \Theta(t_i - t_F) . \quad (17)$$

Here ρ_c is the critical density, defined in Eq. (2), t_F is the network formation time, Γ_k describes the relative emission rate per mode, given by

$$\Gamma_k = \frac{\Gamma}{(3.60)k^{\frac{4}{3}}} , \quad (18)$$

and t_i is obtained by rearranging Eq. (16) to give:

$$t_i(\tilde{t}, f) = \frac{1}{\alpha + \Gamma G\mu} \left(\frac{2k}{f} \frac{a(\tilde{t})}{a(t_0)} + \Gamma G\mu\tilde{t} \right) . \quad (19)$$

As the integral in Eq. (17) runs over all emission times, from the time at which the network is formed to the present time, in order to accurately plot the spectrum, three separate cases need to be accounted for. The first is that in which both the loop is formed and the wave is emitted in the radiation era; the second describes the case in which these events occur in different eras, such that t_i is in the radiation era and \tilde{t} is in

the matter era; and the final case is that in which both the loop is formed and the wave is emitted in the matter era. To encapsulate all three of these cases within the calculated spectrum, the integral in Eq. (17) is split into two integrals, with the first running over times $t \in [t_F, t_{eq}]$, and the second over times $t \in [t_{eq}, t_0]$, where t_{eq} is the time at which radiation-matter equality occurred. These two integrals therefore represent the contributions to the spectrum from the radiation era and matter era respectively. To also consider the case in which t_i and \tilde{t} occur in different eras, it is then necessary to include a conditional statement within the matter era integral, which will change the t_i dependant quantities within the integral depending on whether t_i is greater or less than t_{eq} .

Another consideration that must be taken into account due to these three cases is the fact that the scale factor ratios in both Eqs. (17) and (19) cannot be evaluated in their present state when the numerator and denominator describe different cosmological eras. The scale factor ratios in each era are given by:

$$\frac{a(t_1)}{a(t_2)} = \begin{cases} \left(\frac{t_1}{t_2}\right)^{\frac{1}{2}} ; & t_1, t_2 \in \text{radiation era} \\ \left(\frac{t_1}{t_2}\right)^{\frac{2}{3}} ; & t_1, t_2 \in \text{matter era} ; \end{cases} \quad (20)$$

however, as it is possible for t_i , \tilde{t} , and t_0 to all be in different eras, it is necessary to modify these ratios dependent on the era in which t_1 and t_2 occur. This can be done by splitting the ratio into radiation and matter era specific ratios, and making use of the radiation-matter equality time, resulting in:

$$\frac{a(t_1)}{a(t_2)} = \left(\frac{t_1}{t_{eq}}\right)^{\frac{1}{2}} \left(\frac{t_{eq}}{t_2}\right)^{\frac{2}{3}} ; \quad t_1 \in \text{radiation era}, t_2 \in \text{matter era} . \quad (21)$$

With these considerations it is possible to plot the contributions to the cosmic string gravitational wave background from both the radiation and matter eras, and by then taking the envelope of these curves the total spectrum is obtained.

4.2. Comparison with Detector Sensitivities

Figure 4 shows the power-law integrated sensitivity curves for LISA, LIGO, Einstein Telescope (ET), and Cosmic Explorer (CE). These curves have been generated using an SNR of 10 and an operation time of 4 years. The gravitational wave background produced by a cosmic string network, as generated using the method outlined in the previous section, is also shown on this plot. This curve has been constructed using $G\mu = 10^{-11}$ and $\alpha = 0.1$, as is consistent with recent simulations [4]. The solid orange curve shows the contributions to the total spectrum from gravitational waves emitted in the radiation era and the solid blue curve shows the contributions from the matter era.

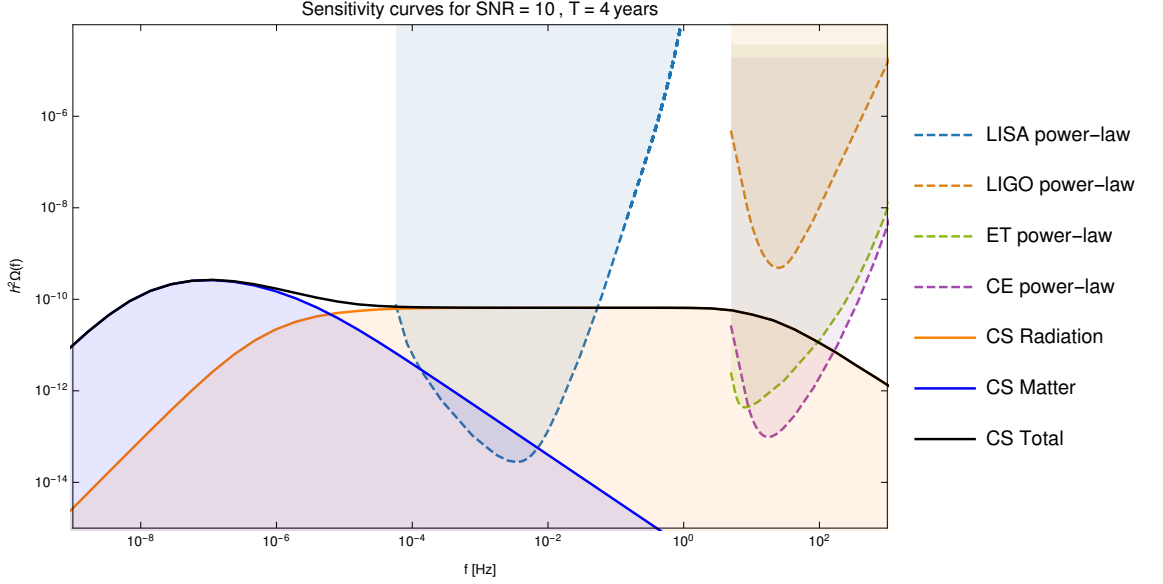


Figure 4: Power-law integrated sensitivity curves for a number of detectors, generated for an SNR of 10 and an operation time of 4 years. Also shown is the theoretical spectrum of a gravitational wave background produced by a cosmic string network. The cosmic string curve has been constructed using $G\mu = 10^{-11}$ and $\alpha = 0.1$, with the contributions to the spectrum from the radiation and matter eras represented by the solid orange and solid blue curves respectively.

It is clear from Figure 4 that the prospects of a detection of the SGWB produced by cosmic strings with the stated characteristics are good, with the SGWB signal lying well above the power-law integrated sensitivity curves for LISA, ET, and CE. Furthermore, the cosmological era in which the gravitational waves were emitted can be seen to greatly alter the resulting SGWB signal. The possibility of a detection is, however, less likely for decreasing values of $G\mu$, as can be seen in Figure 5, which shows the SGWB signal from a cosmic string network for five values of $G\mu$. Clearly, the detectability of the cosmic string spectrum is highly dependent on $G\mu$, such that it will not be possible to detect the signal from a network with $G\mu = 10^{-19}$ at an SNR of 10.

5. Conclusions and Outlook

The detection of the SGWB signal produced by a cosmic string network would provide unprecedented access to the mechanisms of high-energy physics in the early universe. As a new generation of gravitational wave observatories are under construction, the feasibility of the detection of a SGWB of cosmological origin is a matter requiring careful consideration. In this report, the construction of power-law integrated sensitivity curves for gravitational wave detectors was outlined, with the results for LISA, LIGO, ET, and CE presented. These curves demonstrate a significant increase in the sensitivity of the

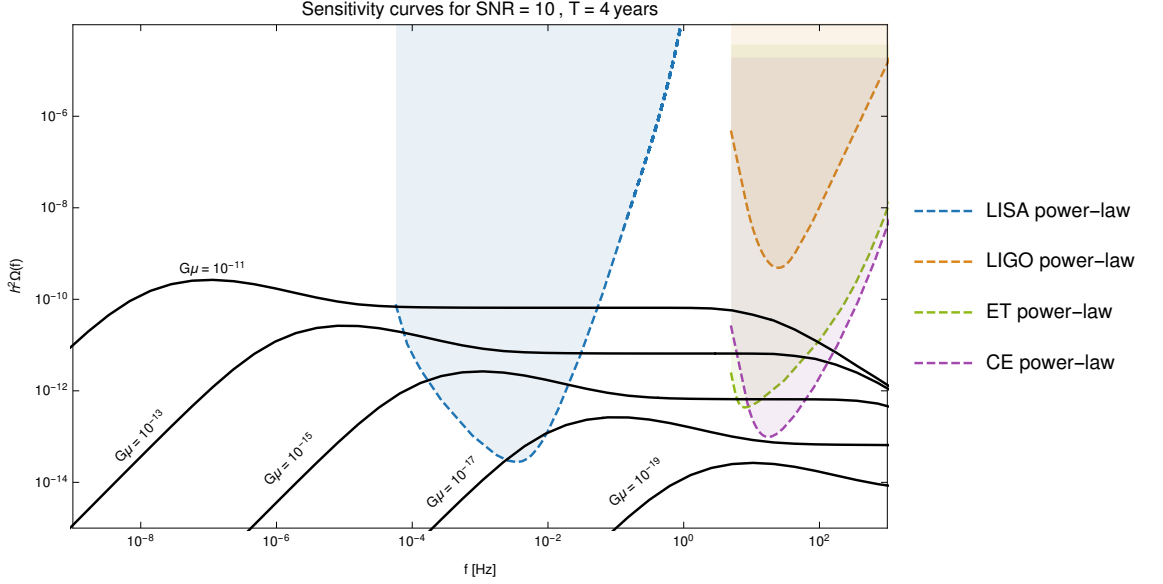


Figure 5: The SGWB signal from a cosmic string network with $\alpha = 0.1$ and $G\mu = 10^{-11}, 10^{-13}, 10^{-15}, 10^{-17}, 10^{-19}$. Also shown are the power-law integrated sensitivity curves for LISA, LIGO, ET, and CE.

detectors, in comparison to the standard method used for sensitivity curve construction. This is due to the fact that the power-law integrated curves take into account the broadband nature of a SGWB signal, a characteristic that is signal dependent and is therefore not necessarily included in the detector sensitivity. This property is taken advantage of through the inclusion of an additional integration over frequency, as was shown for the case in which the SGWB can be described by a power-law spectrum.

The gravitational waves produced by a scaling cosmic string network may provide a predictable SGWB source for detection with upcoming experiments. In the construction of this signal, particular care is required when considering the cosmological era in which the relevant times are situated, as the spectrum is highly dependent on the era in which the gravitational waves were emitted. The theoretical signal from a scaling cosmic string network with $\alpha = 0.1$ and $G\mu = 10^{-11}$ was plotted against the power-law integrated sensitivity curves of the detectors, and it was found that the prospect of detection of such a signal was good for the LIGO, ET, and CE experiments. The dependence of the cosmic string signal is, however, highly dependent on the value of $G\mu$, with smaller values limiting the detectability.

Acknowledgements

I would like to express my utmost gratitude to my supervisors Geraldine Servant and Valerie Domcke, for providing invaluable support throughout the project and making my time here at DESY so interesting and enjoyable. I would also like to thank the rest of the Particle Cosmology group for creating such a friendly atmosphere within which to work, and in particular Yann Gouttenoire, Janis Kummer, and my summer student colleague Anna Kormu, for always being happy to help.

References

- [1] Michele Maggiore. *Gravitational Waves. Vol. 1: Theory and Experiments*. Oxford Master Series in Physics. Oxford University Press, 2007.
- [2] Michele Maggiore. Gravitational wave experiments and early universe cosmology. *Phys. Rept.*, 331:283–367, 2000.
- [3] Bruce Allen and Joseph D. Romano. Detecting a stochastic background of gravitational radiation: Signal processing strategies and sensitivities. *Phys. Rev.*, D59:102001, 1999.
- [4] Eric Thrane and Joseph D. Romano. Sensitivity curves for searches for gravitational-wave backgrounds. *Phys. Rev.*, D88(12):124032, 2013.
- [5] Chiara Caprini et al. Science with the space-based interferometer eLISA. II: Gravitational waves from cosmological phase transitions. *JCAP*, 1604(04):001, 2016.
- [6] Michele Maggiore. *Gravitational Waves. Vol. 2: Astrophysics and Cosmology*. Oxford University Press, 2018.
- [7] Yanou Cui, Marek Lewicki, David E. Morrissey, and James D. Wells. Probing the pre-BBN universe with gravitational waves from cosmic strings. 2018.
- [8] Robert H. Brandenberger, Andreas Albrecht, and Neil Turok. Gravitational Radiation From Cosmic Strings and the Microwave Background. *Nucl. Phys.*, B277:605–620, 1986.
- [9] Yanou Cui, Marek Lewicki, David E. Morrissey, and James D. Wells. Cosmic Archaeology with Gravitational Waves from Cosmic Strings. *Phys. Rev.*, D97(12):123505, 2018.

A. Appendix

In this appendix the power-law integrated sensitivity curves for LIGO, ET, and CE are presented.

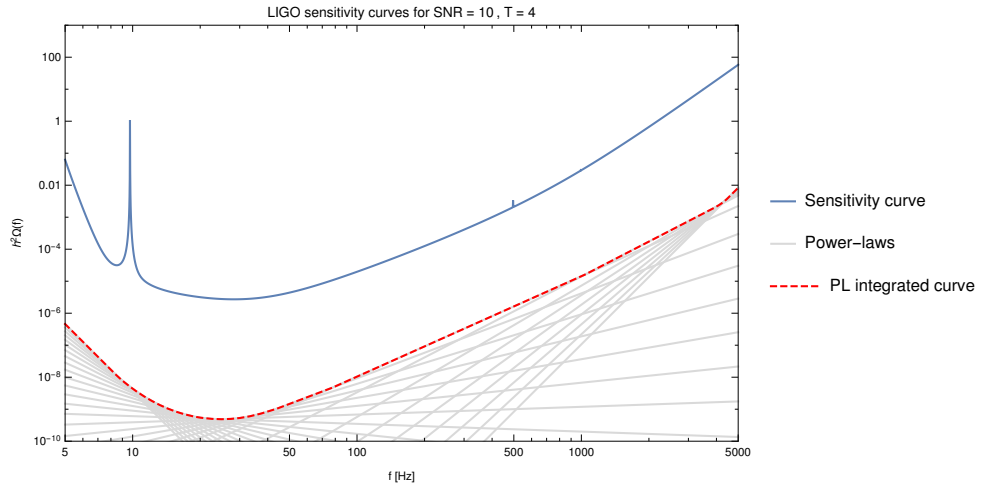


Figure 6: Sensitivity curves for the LIGO experiment, with the power-law integrated sensitivity curve generated for an SNR of 10 and an operation time of 4 years.

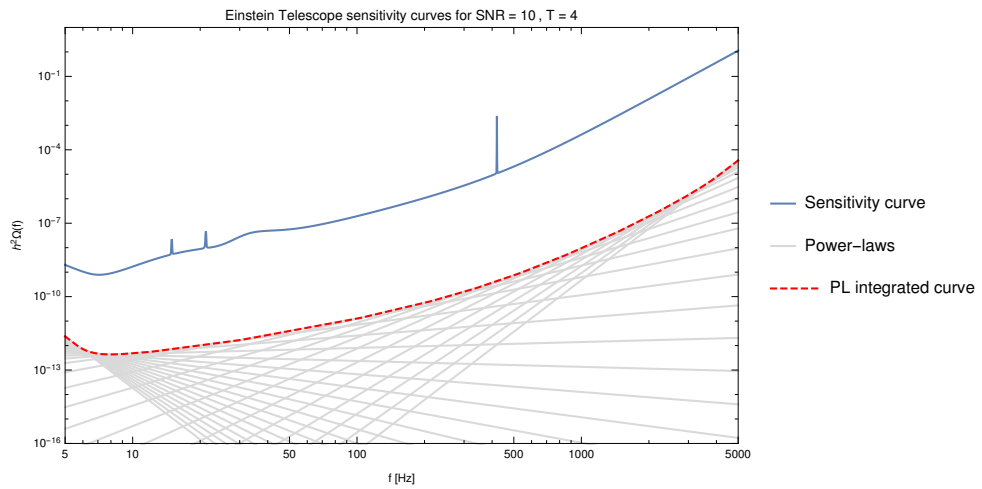


Figure 7: Sensitivity curves for the Einstein Telescope experiment, with the power-law integrated sensitivity curve generated for an SNR of 10 and an operation time of 4 years.

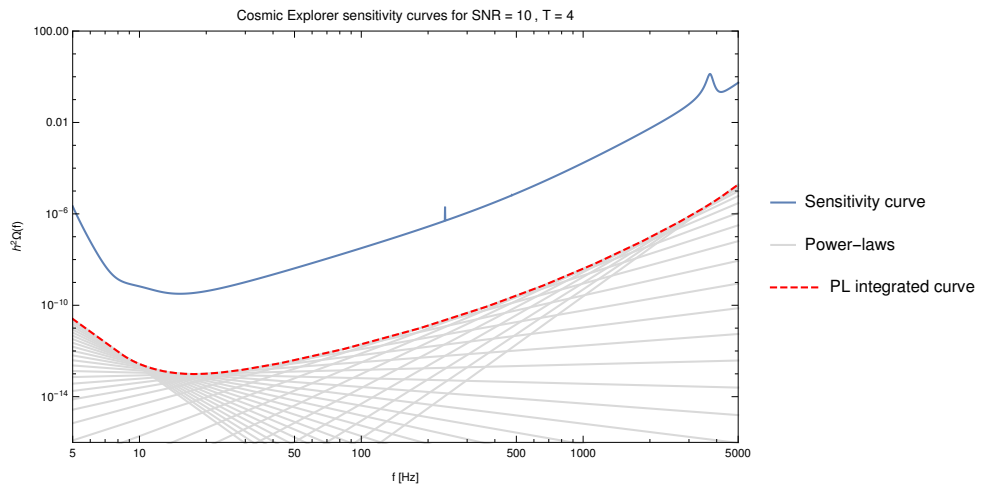


Figure 8: Sensitivity curves for the Cosmic Explorer experiment, with the power-law integrated sensitivity curve generated for an SNR of 10 and an operation time of 4 years.